Photodissociation of ICl Molecule Oriented by an Intense Electric Field: Experiment and Theoretical Analysis

Grégory Bazalgette, Richard White, Gerard Trénec, Eric Audouard, Matthias Büchner, and Jacques Vigué*

Laboratoire Collisions Agrégats Réactivité, I.R.S.A.M.C., Université Paul Sabatier and CNRS U.M.R. 5589, 118, route de Narbonne, 31062 Toulouse Cedex, France

Received: June 25, 1997; In Final Form: November 18, 1997

The idea of orienting molecules by applying an intense electric field on a rotationally very cold molecular beam has been introduced in 1990 by Loesch and Remscheid (*J. Chem. Phys.* **1990**, *93***,** 4779) and also by Friedrich and Herschbach (*Z. Phys. D* **1991**, *18*, 153). Here we describe an experiment in which the orientation thus produced in ICl molecules is tested by a photodissociation experiment. The paper discusses the orientation process with emphasis on the effects nonlinear in the applied electric field. The characterization of the oriented beam and the experiment will be briefly described. A complete simulation leads to a very good fit of the observed signal, but the rotational temperature deduced from this fit is higher than given by a direct measurement, the discrepancy being due to the presence of van der Waals complexes. This experiment has provided the first direct measurement (*Chem. Phys. Lett.* **1995**, *244*, 195) of the sign of the dipole of ICl (I^+Cl^- as expected) and a measurement of the strong orientation achieved.

1. Introduction

A strong orientation of the molecular axis of polar molecules can be produced by applying an intense electric field on a rotationally cold molecular beam. This method was developed by Loesch and Remscheid[1] and it was independently proposed by Friedrich and Herschbach.[2] These pioneering works have opened the way to many new experiments on molecules: reactive[3−5] and inelastic[6] scattering experiments with oriented molecules, spectroscopy of pendular states,[7−12] predissociation of van der Waals complexes,[13,14] ...

This paper presents a description and a complete analysis of an experiment[15] in which the orientation of ICl molecules is measured by photodissociation. The detection of a fragment (here the iodine atom) gives a convenient way of measuring the orientation of the molecular axis before dissociation. This method has been used several times to study the orientation of symmetric-top molecules produced by state-selection techniques[16] and in their first paper on this subject,[2] Friedrich and Herschbach proposed to use photodissociation for measuring the orientation of molecules oriented by an intense field.

The present experiment is also interesting as it has given a direct access to the sign of the dipole moment of ICl in its ground state X, found to be I^+Cl^-, as expected from electronegativity and quantum chemistry arguments.

The content of the paper is organized as follows: in section 2, the theoretical description of orientation process by an intense electric field is completed with emphasis on effects nonlinear in the field. Section 3 discusses the optimization of an oriented molecular beam. Section 4 presents the characterization of our ICl/argon beam. The photodissociation experiment is described in section 5 and its modelization in section 6. Section 7 concludes the paper.

* Address correspondence to this author. Tel: 33 5 61 55 60 16. E-mail: jacques@yosemite.ups-tlse.fr. Fax: 33 5 61 55 83 17.

2. Orientation of a Molecular Beam by an Intense Electric Field

This orientation[1−5] is obtained by introducing a rotationally cold molecular beam in an intense electric field E. When entering the field, the lowest rotational levels $|JM\rangle$ are adiabatically transformed in new eigenstates $|\tilde{J}M\rangle$ which are called pendular states.[7−10]

The orientation which concerns the distribution of the molecular axis must not be confused with the orientation of the angular momentum produced by optical pumping.[17,18] The dimensionless ratio $\omega = \mu E/B$ (μ, dipole moment; B, rotational constant) defines the strength of the orientation effect. Therefore, the average orientation is large if these levels represent a large fraction of the population; *i.e.*, if the rotational temperature T_{rot} is small, $T_{rot} \approx \mu E/k$. Finally, we have verified in a previous paper[19] that the transfer from zero to high field is adiabatic in most cases and that the hyperfine structure has almost no effect on the orientation for ICl.

Almost everything is known about this orientation effect, but some points concerning molecular axis distribution and its nonlinear dependence with the electric field must be clarified. The pendular states $|\tilde{J}M\rangle$ are obtained by diagonalization of the rotational and Stark Hamiltonian given, for a diatomic molecule, by

$$H = B(\vec{J}^2 - \omega \cos\theta) \qquad (1)$$

Various approximate results can be obtained by refined perturbation theory,[20] but the easiest technique, if ω is not too large, is to diagonalize the Hamiltonian matrix on a truncated basis (typically $J_{max} = 20-30$ gives a good description of the levels up to $J_{max}/2$ for ω values less than 20). The diagonalization gives the energies and the wave functions $|\tilde{J}M\rangle$ of the levels. We can thus deduce the distribution $W(\Omega)\, d\Omega$ of the molecular

S1089-5639(97)02074-4 CCC: $15.00
Published on Web 01/23/1998

axis given by

$$W(\Omega)\,d\Omega = \sum_{\tilde{J}M} P(\tilde{J},M)|\langle\Omega|\tilde{J}M\rangle|^2\,d\Omega \qquad (2)$$

One usually assumes that the population of the level $|\tilde{J}M\rangle$ is given by the Boltzmann distribution of the corresponding zero field level $|JM\rangle$:

$$P(J,M) = \frac{1}{Z}\exp-\left(\frac{BJ\,(J+1)}{kT_{\rm rot}}\right) \qquad (3)$$

with the partition function $Z = \sum_J(2J+1)\exp[-(BJ(J+1)/kT_{\rm rot})]$. The axis distribution $W(\Omega)$ depends on three energetic quantities B, μE, and $kT_{\rm rot}$ and for homogeneity reasons only on two ratios $\omega = \mu E/B$ and $y = B/kT_{\rm rot}$. All the following calculations have been made for $I^{35}Cl$ ($B = 3414.366$ MHz,[21,22] $\mu = 1.207 \pm 0.003$ D[23]), but they apply to any other problem described by the same values of the dimensionless parameters ω and y. We concentrate on the case of small y values. The opposite case (*i.e.*, $B \gg kT_{\rm rot}$) corresponds to light molecules with large B values for which it is difficult to obtain a large orientation effect.

The partition function is given very accurately by an approximate formula[24]

$$Z = \frac{1}{y} + \frac{1}{3} + \frac{y}{15} + \ldots \qquad (4)$$

The axis distribution $W(\Omega)\,d\Omega$ has always cylindrical symmetry and depends only on the angle θ between the field and the molecular axis. In low field ($\omega \le 1$), a perturbation calculation up to the first order gives

$$W(\Omega) = \frac{1}{4\pi}\left(1 + \frac{\mu E}{BZ}\cos\theta\right) \qquad (5)$$

which is equivalent to the classical distribution if $y \ll 1$:

$$W(\Omega) \propto \frac{1}{4\pi}\exp\left(\frac{\mu E}{kT_{\rm rot}}\cos\theta\right) \qquad (6)$$

The orientation O is the average value of $\cos\theta$. Its classical value $O_{\rm cl}$ in low field is $O_{\rm cl} \approx \mu E/3kT_{\rm rot}$ while the quantum average in low field is $O = \mu E/3BZ \approx \mu E/3kT_{\rm rot}$ if $y \ll 1$. We have calculated the orientation O given by

$$O = \sum_{JM} P(\tilde{J},\,\mathrm{M})\langle\tilde{J}M|\cos\theta|\tilde{J}M\rangle \qquad (7)$$

and also the distribution $W(\Omega)$ numerically for various rotational temperatures as a function of the field. First, we have tried to see how the orientation saturates when the field becomes large. Figure 1 presents a plot of $O/(\mu E/3kT_{\rm rot})$ as a function of $\mu E/kT_{\rm rot}$. The curve is almost independent of the value of the rotational temperature (*i.e.*, of the quantity y), but its shape differs strikingly from the classical result given by $O_{\rm cl}$, in particular because the classical and quantum calculation describe different situations: the classical calculation assumes the thermodynamic equilibrium in the field while the present quantum calculations assume equilibrium in zero field and adiabatic transfer in the field region.

It may be strange that the calculated curves do not converge to unity in zero field and that their ordering is such that at a given electric field strength, the lower the rotational temperature, the lower is its ratio $O/O_{\rm cl}$. These effects are coming from the expansion of the partition function Z in low field. The

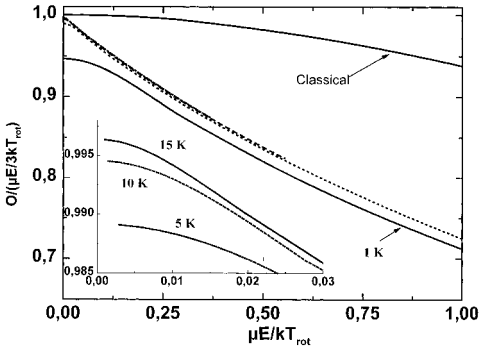

Figure 1. Plot showing the saturation of the orientation of ICl with the field. In the linear regime, the classical formula giving the orientation is $O_{\rm cl} = \mu E/3kT_{\rm rot}$ so that the plot of $O/(\mu E/3kT_{\rm rot})$ will reveal the deviations from the linear regime and from the classical formula. The full curve labeled "classical" is the exact classical formula (see ref 19, eq 12). The other curves are the results of our quantum calculations for temperatures $T_{\rm rot} = 15$ K (dot-dash), 10 K (dash), 5 K (dot), and 1 K (full). Except the last one, they are almost indistinguishable. Surprisingly, the saturation appears to be almost a linear function of the field, although simple arguments prove that it should be quadratic: this quadratic behavior is well verified by an expanded view of the low-field part of these curves (see insert). Finally, our experiment samples the range of $\mu E/3kT_{\rm rot}$ up to 0.66 (corresponding to $E = 7$ MV/m and $T_{\rm rot} = 3$ K).

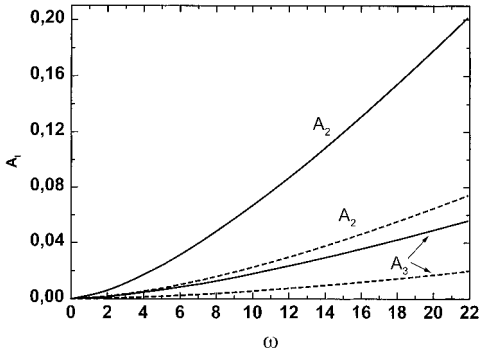

Figure 2. Plot of the first ($l = 2$ and 3) A_l parameters (defined by eq 10) for $T_{\rm rot} = 3$ K (full curves) and $T_{\rm rot} = 6$ K (dashed curves). Their values are not negligible as soon as $\omega > 5$ and as expected, their behavior is nonlinear with E and with $T_{\rm rot}^{-1}$: in particular, we have verified that in low field, A_2 is proportional to ω^2 and A_3 to ω^3.

calculated orientation is given by $O = \mu E/3BZ \approx \mu E/(3kT_{\rm rot} + B)$ using eq 4. Consequently, the ratio $O/O_{\rm cl}$ behaves as $1/(1 + B/(3kT_{\rm rot}))$ for vanishing field strength. This expression is always lower than unity and also explains the observed ordering.

Obviously, the orientation O does not give a complete description of the distribution $W(\Omega)$ as soon as the field is not very weak. This effect has already been discussed for CH_3I by Bulthuis et al.[25] using an expansion of $W(\Omega)$ in Legendre polynomials:

$$W(\Omega) = \frac{1}{4\pi}\left(\sum_{l=0} A_l P_l\,(\cos\theta)\right) \qquad (8)$$

and such a description was used by Van Leuken *et al.*[26] to analyze the reactive collision of oriented CH_3Br. $A_0 = 1$ because of normalization and obviously, $A_1 = 3O$.

We present in Figure 2 the values of A_2 and A_3 as a function of the reduced field parameter ω for two rotational temperatures: it is important to remark that these parameters are nonlinear functions of ω. For ω values greater than 10, as reached in our experiment, this more refined description of $W(\Omega)$ is absolutely necessary as the values of higher order parameters

TABLE 1: Values of the Terminal Speed Ratio $S_{\parallel\infty}$ for a Supersonic Beam of Pure Rare Gases at $p_0d = 5.7$ Torr·cm and $T_0 = 300$ K Values of the Rotational Temperature T_{rot} of ICl Seeded in the Same Rare Gas Measured by LIF for the Same Source Conditions

gas	He	Ne	Ar
$S_{\parallel\infty}$	12[b]	16[c]	22[c]
$T_{\parallel}$ (K)[a]	5.6	2.8	1.5
T_{rot} (K)	5.0[d]	2.6[d]	1.6[d]

[a] The parallel temperature is calculated from $S_{\parallel\infty}$. [b] From refs 33 and 37. [c] From ref 38. [d] From ref 35.

A_2, A_3, ... are not negligible, even though the most important and interesting effect is the orientation (for instance, an alignment $A_2 \neq 0$ can be obtained by supersonic expansion, see ref 27 and references therein).

An interesting point concerns the molecular axis distribution $W(\Omega)$ for $\theta = 0$, as this is the quantity that an ideal experiment would measure. Its value is given by $W(\theta = 0) = (\sum_l A_l)/4\pi$. The simplest description limits this quantity to the $l = 1$ term and then $W(\theta{=}0) = (1 + A_1)/4\pi$: the saturation effect discussed in Figure 1 shows that this approximate form predicts that $W(\theta{=}0)$ increases with the field less rapidly than linearly. But, the exact calculation shows the opposite behavior. In fact, this calculation includes the higher l values (A_2, A_3, ...), which increase more rapidly than linearly with the field and overcompensate the A_l term. Accordingly, $W(\theta{=}0)$ must increase more rapidly than linearly. This nonlinear effect is well observed in our experiment, although it is not ideal.

3. Optimization of an Oriented Molecular Beam of ICl

This optimization differs from the usual optimization of a supersonic molecular beam. The goal is not only to have an intense beam, but one needs also a very low rotational temperature without too many van der Waals complexes.

a. The $\mathscr{T}_{ICl}O^2$ Criterion. In our previous paper,[19] we have recalled the well-known argument originally developed for spin $^1/_2$ oriented targets. The best signal to noise ratio of an experimental effect due to the orientation is obtained if the product of the particle density times the square of their orientation O is maximum. The density being proportional to the partial beam intensity $\mathscr{T}_{ICl}$, the optimization must aim at maximizing the $\mathscr{T}_{ICl}O^2$ product. As shown in section 2, in most cases of experimental importance, the orientation O can be roughly (with a 20 or 30% error at most) estimated from its classical value $O_{cl} = \mu E/3kT_{rot}$ We have to maximize the electric field E by a proper design of the electrodes (material, shape, spacing, and surface treatment[28]) and the quantity $\mathscr{T}_{ICl}/T_{rot}^2$ by adjusting the source parameters of the molecular beam. Only this second part of the optimization is discussed here.

b. Molecular Beam Optimization. The beam must be very intense, rotationally very cold, and the polar molecules must remain free; *i.e.*, only a small fraction may be bound in van der Waals complexes, because the orientation and reaction dynamics properties of these complexes are quite different from those of free molecules. Finally, as ICl decomposes in $I_2 + Cl_2$ at elevated temperatures,[29,30] the source temperature T_0 should remain close to 300 K (the partial pressure of ICl is then a few tens of mbars). We have worked only with argon as a carrier gas because helium is not very favorable to produce very low rotational temperatures (Table 1) and neon is expensive. Using the theory of supersonic beams, we optimize the free parameters which are the total source density n_0 and the nozzle diameter d. We assume that the dilution of ICl is sufficient to perturb only weakly the expansion properties of the carrier gas.

The intensity $\mathscr{T}$ of a supersonic beam of a pure monoatomic gas and the total number of atoms emitted per unit time $\dot{N}$ both scale like n_0d^2 (see ref 31). For ICl seeded in the rare gas, the partial intensity $\mathscr{T}_{ICl}$ is then given by

$$\mathscr{T}_{ICl} = \mathscr{T}(n_0^{ICl}/n_0)\Phi \tag{9}$$

where n_0^{ICl} is the ICl density in the source ($n_0^{ICl} \ll n_0$) and Φ is an enrichment factor[32] which tends toward m_{ICl}/m_0 in the limit of large p_0d values. We assume that this limit is reached. The parallel temperature $T_{\parallel}$ of the beam is given by[33]

$$T_{\parallel} \approx \frac{\gamma T_0}{(\gamma - 1)S_{\parallel\infty}^{\ 2}} \tag{10}$$

where T_0 is the source temperature and $S_{\parallel\infty}$ the terminal value of the parallel speed ratio,[33] which scales with the source density and nozzle diameter like $(n_0d)^{0.53}$. The rotational temperature T_{rot} of ICl seeded in rare gases has been measured by several authors[34,35] and appears to be very close to the parallel temperature of the pure rare gas beam operated at the same p_0d value.[33,36−38] This information is collected in Table 1. We will therefore assume that $T_{rot} = T_{\parallel}$. We can now evaluate the dependence of the product $\mathscr{T}_{ICl}T_{rot}^{-2}$.

$$\mathscr{T}_{ICl}T_{rot}^{\ -2} \propto n_0^{ICl}n_0^{\ 2.12}d^{4.12} \tag{11}$$

If the product n_0d^2 was limited by the available pumping speed, then $\mathscr{T}_{ICl}T_{rot}^{-2}$ would scale as $d^{-0.12}$ and this would slightly favor working at high n_0 and small d values. However, when condensation begins, the terminal speed ratio goes through a maximum for a source density n_c which scales as $d^{-0.55}$ following Meyer.[38] Near n_c, the $\mathscr{T}_{ICl}T_{rot}^{-2}$ quantity should scale as $d^{2.95}$. Finally, the formation of ICl−rare gas van der Waals complexes must concern at most a small fraction of ICl molecules, and this complex formation occurs for lower source density than condensation. In the supersonic beam the fraction of ICl molecules engaged in a complex with rare gas atoms should scale with the source density and nozzle diameter in a way similar to the fraction of rare gas dimers in a pure rare gas beam. Following Knuth,[39] this last fraction scales as $n_0^{5/3}d^{2/3}$ in very good agreement with experiments.[40] Then, if one works at a fixed concentration of ICl−rare gas complexes, the density n_0 scales as $d^{-0.4}$ and the $\mathscr{T}_{ICl}T_{rot}^{-2}$ quantity should scale as $d^{3.27}$.

These last considerations prove that the optimum of the quantity $\mathscr{T}_{ICl}T_{rot}^{-2}$ is obtained with a small source density n_0 and a large nozzle diameter d. However, d must not be too large so as to keep the total density n_0 larger than n_0^{ICl} and also to produce a low rotational temperature.

4. Characterization of Our ICl−Argon Beam

The experiment was performed in our crossed beam machine already described[41] and the modifications done for the present experiment are described in our previous paper.[15]

The molecular beam has been characterized by laser-induced fluorescence detection of ICl on the A−X $v' = 21 - v'' = 0$ transition. The laser system, the optics for fluorescence collection, the photomultiplier, and the electronics have already been used to study the spectroscopy of the pendular states of ICl.[11,12] A small modification is the introduction of a fiber bundle between the collection optics and the photomultiplier.

The laser-induced fluorescence spectra were very similar to the ones observed in zero field during our previous experi-

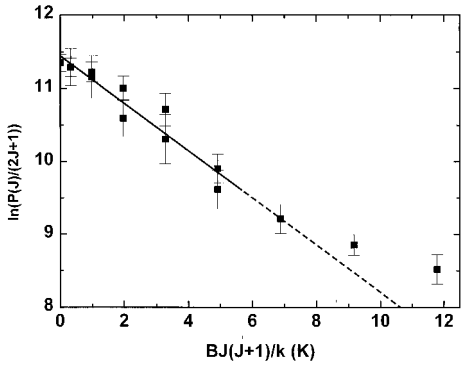

Figure 3. Boltzmann plot of the population of the X $^1\Sigma^+_0$, $v = 0$, low J levels of ICl measured by LIF (only Q and R line data have been included). ln[$P(J)/(2J + 1)$] is plotted as a function of the rotational energy $BJ(J + 1)/k$ expressed in Kelvin. This experiment has been done with the parameters chosen as optimum: $p_0 = 150$ mbar, $d = 280$ μm, nozzle−skimmer distance $z_s = 15$ mm. The temperature deduced from this plot is $T_{rot} = 3.08 \pm 0.26$ K (the last three points have not been included in the fit). The population of the highest J levels ($J = 7$ and 8) exceeds the calculated values.

ment.[11,12] In particular, the residual Doppler broadening is also of the order of 10 MHz and the laser power is sufficient to saturate slightly the excitation process, a condition which is not favorable to simplify the analysis. We used a computer program to simulate the intensity of the various hyperfine components. From the comparison of observed and simulated spectra, we have deduced the population $P(J)$ of the ground state level X $^1\Sigma^+_0$, $v = 0$, J. A Boltzmann plot is presented in Figure 3. Usually, we measured only the population of the levels $J = 0-5$ (each measurement requiring a few minutes long laser scan over the whole hyperfine structure of the corresponding line). We have also measured during two runs the population of higher J levels ($J = 6-8$). As usual (ref 42 and references therein), the population of these higher J levels is substantially larger than predicted from a Boltzmann extrapolation. We discuss here only the low-J population. A point that we do not understand is that the population measurements based on P lines give a larger population than those based on Q and R lines. However, these two sets of lines, when fitted independently, give good fits with consistent values of the rotational temperature. We have measured the rotational temperature for various source pressures p_0 (50−1000 mbar) and nozzle diameters d (90, 170, and 280 μm). The stainless steel skimmer is located at a distance $z_s = 15$ mm from the nozzle (we have tried a smaller distance $z_s = 8$ mm, but the beam properties indicated that skimming at high intensity is not perfect).

Figure 4 presents a plot of our measurements of the rotational temperature as a function of the product p_0d. We compare our values to those measured by Keil et al.[34] and Hansen et al.,[35] and also to the parallel temperature of a pure argon beam.[38] All these temperatures are very close. The low values obtained by ref 34 may be due to their different measurement technique (based only on the $J = 0$, 1, 2 populations). Our values are significantly higher than the one of ref 35, but we used a higher concentration of ICl than Hansen et al., who noticed that T_{rot} increases with ICl concentration.

The intensity of the LIF signals due to the very low J levels ($J = 0$ and 1) have another interest: because the rotational energies of these levels are below kT_{rot}, these signals are proportional to $\mathcal{T}_{ICl}/Z$ or $\mathcal{T}_{ICl}/T_{rot}$ a quantity close to the one we want to optimize. More important, these LIF signals distinguish ICl from ICl complexes, while the mass spectrometry signals (not presented here) do not, because of fragmentation

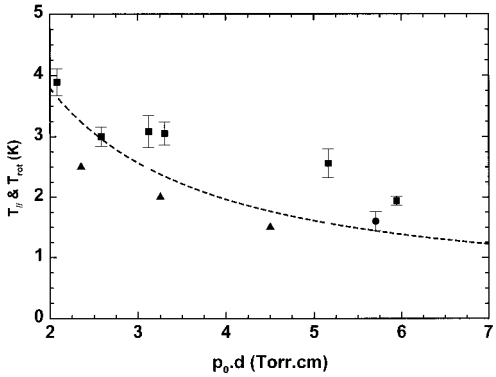

Figure 4. Plot of the parallel temperature $T_{||}$ (in kelvin) of a pure argon beam (full curve deduced from the data of Meyer[38]) and of the rotational temperature T_{rot} (in kelvin) of ICl seeded in argon as a function of the product p_0d expressed in Torr·cm: triangles are data of Keil et al.,[34] circles are data of Hansen et al.,[35] squares are present work. $T_{||}$ and T_{rot} are clearly very close, and the differences between the various measurements of T_{rot} are partly due to the technique and partly because T_{rot} increases with the seeding ratio n_0^{ICl}/n_0.

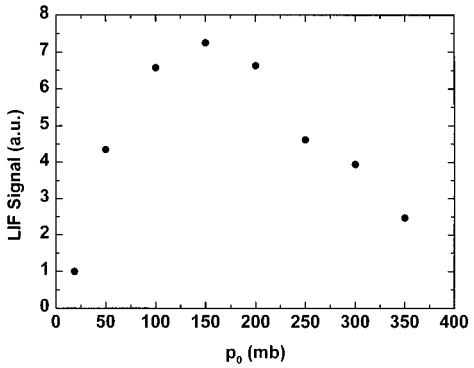

Figure 5. Plot of the LIF signal of the low J levels (sum of the signals of $J = 0$ and 1) as a function of the source pressure p_0. The rapid increase when $p_0 < 150$ mbar is mostly due to rotational cooling and enrichment of the heavy species on the expansion axis while the decrease for $p_0 > 150$ mbar is due to the formation of van der Waals complexes containing ICl (ICl−Ar, $(ICl)_2$).

during ionization. Figure 5 presents the behavior of the low J LIF signal with the total source pressure p_0. The total ICl content of molecular beam measured by mass spectrometry appears almost independent of the total source pressure. The intensity of the low J LIF signal can be expressed as $(1 - x_{vdw})T_{rot}^{-1}$ where x_{vdw} is the molar fraction of ICl in van der Waals complexes. As T_{rot} is expected to behave like $p_0^{-1.06}$, the rapid decrease of this signal when p_0 is larger than 150 mbar is due to the rapid increase of the complexed fraction x_{vdw}. If this fraction behaves like $p_0^{5/3}$ (see section 3), the maximum occurs when $x_{vdw} \approx 0.3$. We do not expect this estimation to be quantitative but it clearly suggests the importance of these complexes in the beam. Our experimental choice was to do the photodissociation experiment in these conditions ($p_0 = 150$ mbar, $d = 280$ μm), corresponding to a rotational temperature $T_{rot} = 3$ K. In these working conditions, the dilution of ICl is rather high (12%) and the throughput of the pump is not a limitation. This choice leads to a very intense and very cold beam, but we probably underestimated the importance of ICl complexes.

5. Photodissociation of Oriented ICl Molecules

a. Description of the Photodissociation Continuum. Several photodissociation studies of ICl have been made[43−45]

but we are interested here only in the visible range. We considered that it was highly probable to initiate electrical breakdown in the condenser using intense UV pulses and we choose to use a CW laser in the visible range as photodissociation source. The absorption continuum of ICl[46] is maximum near $\lambda = 470$ nm ($\epsilon = 111.4$ mol^{-1} L^{-1} cm^{-1}) but the absorption is only slightly less intense at $\lambda = 490$ nm ($\epsilon = 95.0$ mol^{-1} L^{-1} cm^{-1}) so that the natural choice is to use the intense 488 nm line of the Ar^+ laser. The work of De Vries et al.[43] has given a very complete characterization of this photodissociation process. The transition is almost a purely parallel B 0^+-X 0^+ transition and the photodissociation products are I + Cl (21%) and I + Cl* (79%) when 490 nm photons are used.

The wavenumber of the Ar^+ 4p $^2D_{5/2}-4s\ ^2P_{3/2}$ 488 nm line is 20 486.69 cm^{-1}.[47,48] The dissociation energy of $I^{35}Cl$ D_0 is 17 365.804 cm^{-1} [49] and the $^2P_{1/2}-^2P_{3/2}$ splitting in chlorine atom is found to be 882.352 cm^{-1}.[50] We can thus calculate the recoil energies for the two photodissociation channels, 3121 and 2239 cm^{-1}, and the corresponding relative velocities $v_r = 1650$ m/s and $v_r^* = 1398$ m/s. The recoil velocities of the iodine atom in the center of mass frame are equal to $u_I = 356.5$ m/s; $u^*_I = 301.9$ m/s for ^{35}Cl (respectively $u_I = 364.3$ m/s and $u^*_I = 308.5$ m/s for ^{37}Cl).

b. Theoretical Description of the Photodissociation Process. The general theory of photodissociation in the presence of an intense field should be quite complex. However, for a direct photodissociation process the dissociation occurs in a very brief time τ_{diss}. It can be roughly evaluated using classical mechanics, $\tau_{diss} \approx 2 \times 10^{-13}$ s. The Stark Hamiltonian H_s is too weak to play a role during this short time. More precisely, the sudden approximation[51] can be applied because

$$H_s \tau_{diss} \ll \hbar \tag{12}$$

With μ of the order of 1 D and $E = 7$ MV/m (*i.e.*, our maximum applied field) $\mu E \approx 2.3 \times 10^{-23}$ J, this condition can be written

$$\tau_{diss} \ll 5 \times 10^{-12}\ \text{s} \tag{13}$$

well fulfilled by our estimated value of τ_{diss}. This discussion may take a more obvious form. It is clear that if the photodissociation process was going through a Rydberg state or an ionic molecular state (of the I^+Cl^- type for instance), the large external electric field could strongly modify the dissociation dynamics. But here, the dissociation goes through an excited state which has a mixed covalent−ionic nature near the ground state equilibrium distance and becomes rapidly purely covalent when the atoms separate (this behavior appears very clearly on the vibrational dependence of the dipole moment of the A state[23,52]). The Stark shift of the excited state has been estimated of the order of 1 cm^{-1}, and this quantity must be compared to the width of the dissociation continuum equal to several thousand of cm^{-1}.[46]

The axial recoil approximation is the basic description of a direct dissociation process.[53,54] This approximation should be excellent here because of the very low rotational temperature. A classical mechanics calculation can be used to estimate the angle of rotation α of the molecular axis during dissociation:

$$\alpha = \beta[E_{rot}/E_{recoil}]^{1/2} \tag{14}$$

where β is a constant of the order of unity depending of the shape of the repulsive potential curve. With the present recoil energies E_{recoil} and rotation energies $E_{rot} = kT_{rot}$, the angle α is estimated in the range 0.02−0.04 rad, a clearly negligible effect.

Under these approximations, we may write the angular distribution of the fragments $I(\Omega)\,d\Omega$ as the product of the initial distribution of molecular axis $W(\Omega)$ by the probability of photodissociation $P(\Omega)$. This type of argument has already been developed by Zare,[55] Friedrich and Herschbach[2] and Taatjes et al.:[56]

$$I(\Omega)\,d\Omega = W(\Omega)\,P(\Omega)\,d\Omega \tag{15}$$

$W(\Omega)$ depends only of the angle θ_S between the static field and the molecular axis. $P(\Omega)$ depends only of the angle θ_L between the laser field and the molecular axis. $P(\Omega) = \cos^2\theta_L$ (or $\sin^2\theta_L$) for a parallel (or perpendicular) transition. We assume that the transition is purely parallel and we have used a laser field parallel to the static field because this choice gives the maximum signal. The choice of a laser polarization perpendicular to the static field would lead to a vanishing signal in the axial recoil approximation for a purely parallel transition (we verified experimentally that the signal was considerably reduced in this second case). Then the formula of the distribution of the product in the center of mass frame is very simple ($\theta = \theta_S = \theta_L$):

$$I(\Omega)\,d\Omega = W(\Omega)\cos^2\theta\,d\Omega \tag{16}$$

with $W(\Omega)$ given by eq 8.

c. Experimental Arrangement. We have chosen to detect the iodine atomic fragment for the following reasons. Because its recoil velocities are less than the mean velocity of the molecular beam ($v_{ICl} = 498.1$ m/s), there is not a one-to-one correspondence between the center of mass frame and the laboratory frame (see the corresponding Newton diagram in Figure 3 of our previous paper[15]). Nevertheless, the photodissociation signal is a good tool to measure the orientation: using eq 19 below, we have calculated the cos θ value averaged over the detected atoms $\langle\cos\theta\rangle = 0.922$ not far from unity which would correspond to an ideal experiment.

The choice of detecting the iodine fragment was dictated by the poor differential pumping of the mass spectrometer. The ICl density in the ionizer is sufficient to induce a large background so that we have to fully optimize the detected signal, and iodine at mass 127 presents many advantages. There is no other background peak nearby which makes it possible to enhance the signal by diminishing the resolution of the spectrometer. The ionization cross section is expected to be larger for iodine than for chlorine.[57,58] Two kinematic effects enhance the signal: the iodine atoms are concentrated in a cone around the ICl beam and their lab velocity is smaller than that of chlorine atoms. The photodissociation setup has already been described (see ref 15).

d. Results. The photodissociation signal $S(E)$ was extracted from the background by modulating the laser beam and detecting the resulting modulation of the ion signal by a lock-in detector (for details see ref 15). The zero-field signal $S(0)$ is used for normalization and the signal thus defined as the ratio $S(E)/S(0)$ is plotted in Figure 6.

Our first comment concerns the sign of the effect. From the known polarity of the high voltage plates, we have deduced[15] that the sign of the dipole moment of ICl in its X state is I^+Cl^- in agreement with electronegativity and quantum chemistry arguments. From the experimental point of view, it appears that it is very difficult to measure directly a sign of a molecular dipole moment (the case of the CO X state dipole moment is very interesting in this respect[59−61]). An indirect measurement can be deduced from the hyperfine coupling constants.[62] In particular, with halogen and interhalogen molecules, the hy-

perfine quadrupolar term is sensitive to the holes in the p shell: this quantity increases when going from $X(np)^5$ to $X^+(np)^4$ and decreases when going from $X(np)^5$ to $X^-(np)$.[6,63−65,66] This argument fits very well the observation in this family of molecules, but strangely it would suggest a nonpolar character of iodine in ICN molecule (the quadrupolar coupling constant of ^{127}I nucleus in this molecule, −2420.2 MHz,[67] is very close to the value in $^{127}I_2$ molecule, −2452.6 MHz[68]).

6. Monte Carlo Simulation of the Experimental Signal

a. The Monte Carlo Calculation. We have developed a Monte Carlo simulation of the experiment in order to evaluate the experimental signal given by eq 16. The molecular beam is described in a somewhat simplified manner: the molecules are assumed to follow straight line trajectories coming from the center of the nozzle, distributed with an equal probability over the collimating aperture. The normalized velocity flux density is given by[69]

$$f(v) = Nv^3 \exp\left[-\left(\frac{v - v_{ICl}}{\alpha}\right)^2\right] \quad (17)$$

$v_{ICl} = 498.1$ m/s has been calculated by the theory of supersonic expansions including the effect of seeding on the initial enthalpy and average molecular mass, $\alpha = [2KT_{||}/m_{ICl}]^{1/2} = 17.5$ m/s (using $T_{||} = T_{rot} = 3$ K).

The photodissociation occurs anywhere in the intersection volume of the molecular and laser beams, the probability of this event being proportional to the laser intensity I_L, assuming a Gaussian laser beam ($I_L = I_0 \exp(-2\rho^2/w^2)$ with $w = 1$ mm and ρ the distance to the laser beam axis).

The initial orientation of the ICl molecule being random, the Monte Carlo procedure calculates the signal $S(E)$ in the following form:

$$S(E) = \sum_l A_l \langle P_l(\cos\theta)\rangle \quad (18)$$

A_l are calculated as described in section 2 and we have taken into account the terms $l = 0$ up to 5. The brackets designate the average over the atoms which go through the ionizer. This average can be written as

$$\langle P_l(\cos\theta)\rangle = \sum_{i=1}^{4} \int d^3\vec{r} \int dv\, f(v) \int d\Omega\, I_L(\vec{r})\, D(\vec{r}, v, u_i, \theta, \varphi)\, P_l(\cos\theta) \cos^2\theta \quad (19)$$

The $\cos^2\theta$ factor is the photodissociation probability assuming a purely parallel transition. $D(\vec{r}, v, u_i, \theta, \varphi)$ is a detection function equal to 1 or 0 depending on whether the atom trajectory goes through the ionizer or not: It depends on the initial position $\vec{r}$ and orientation of the molecule (given by θ and φ) and of the final iodine atom velocity obtained as the vectorial sum of the initial velocity of ICl and of the recoil velocity of the iodine atom (this velocity u_i can have four different values discussed above). We verified that replacing this step function by an ionization probability proportional to the time spent in the ionizer has very little effect on the averages. The present formulation (eq 18) splits the problem in two parts: (1) the detection geometrical effects which are calculated in the average of the $P_l(\cos\theta)$, and (2) the molecular axis distribution which appear only through the A_l (which are functions of the field E and the rotational distribution).

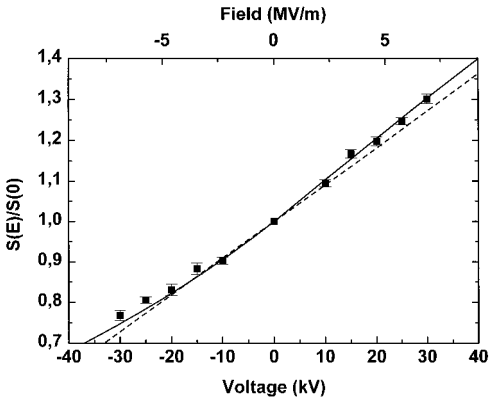

Figure 6. Experimental results $S(E)/S(0)$ as a function of the applied voltage in kV (lower scale) and the estimated electric field in MV/m (upper scale). Two fits are presented: (1) a linear function (eq 20), $S(E)/S(0) = 1 + \gamma E$ (dashed curve). Clearly, systematic deviations appear which are due to the neglected nonlinear dependence of $W(\Omega)$ with the electric field. The rotational temperature deduced from this fit is $T_{rot} = 7$ K; (2) a second fit uses Monte Carlo modelization of the experiment (full curve). The description of the molecular axis distribution is made using eq 8 which takes into account the nonlinear effects with the electric field but the rotational distribution is described by only one temperature, $T_{rot} = 6$ K.

b. The Results. In the first step we may verify that the complete description of $W(\Omega)$ is necessary. If we use the simplified theoretical description of $W(\Omega)$ given by eq 5, the dependence of $S(E)/S(0)$ with E is given by

$$S(E)/S(0) = 1 + \gamma E \quad (20)$$

We have fitted this very simple formula to the data. The straight line resulting from this fit (Figure 6) passes below almost all the experimental data points. This proves clearly the importance of effects nonlinear with the field E and in the following calculations we have taken into account the A_l coefficients with $l = 0-5$.

We can easily fit the rotational distribution to give the best representation of the observed data points. This was done using either a single Boltzmann distribution (eq 3) or the sum of two normalized Boltzmann distributions at temperatures T_1 and T_2:

$$P(J,M) = \frac{W_1}{Z_1} \exp\left[-\left(\frac{BJ(J+1)}{kT_1}\right)\right] + \frac{W_2}{Z_2} \exp\left[-\left(\frac{BJ(J+1)}{kT_2}\right)\right] \quad (21)$$

W_1 and W_2 are the weights ($W_1 + W_2 = 1$).

The best fit with one rotational temperature was obtained for a rotational temperature $T = 6$ K (Figure 6). This fit is considerably better than a straight line fit as given by eq 30 but some discrepancies remain for negative voltages. Moreover, the rotational temperature deduced from this fit is an effective value, far from our LIF measurement.

A series of curves obtained for a two temperatures rotational distribution is presented in Figure 7. The temperatures have been fixed at $T_1 = 3$ K (the observed value deduced from LIF) and $T_2 = 15$ K (the sensitivity of the fit to the exact value of the high temperature is low) and we have only varied the weights W_1/W_2. A very good fit is obtained with weights equal 40−60%. The weight for the low-temperature distribution is lower than expected. The most obvious explanation is that this is due to some neglected effects which are thus effectively represented. From the data of Figure 5, it seems probable that an important fraction of ICl molecules are bound in van der Waals complexes (ICl−Ar, $(ICl)_2$). These complexes behave very differently from

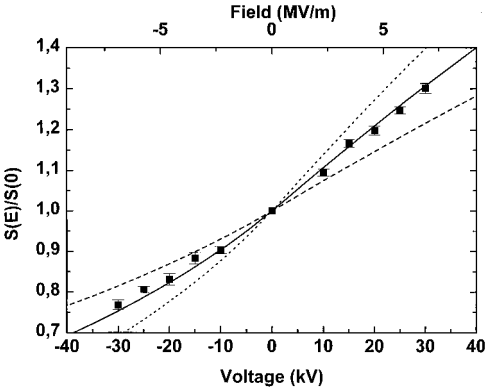

Figure 7. Same fit as in Figure 6 but with a two-temperature model. We have chosen the lower temperature $T_1 = 3$ K following our LIF measurement of the low J population and we have found that the fit is not very sensitive to the choice of the higher temperature (here $T_2 = 15$ K). Several curves obtained with different weights have been plotted: dashed curve → $W_1 = 0.2$, $W_2 = 0.8$; full curve → $W_1 = 0.4$, $W_2 = 0.6$; dotted curve → $W_1 = 0.6$, $W_2 = 0.4$. Our data is well explained by the model with $W_1 = 0.4$, $W_2 = 0.6$. Although we are convinced that there is excess population at high J, we would not expect such a large contribution of the higher temperature distribution. This contribution describes in an effective manner various effects, the most important being probably the contribution to the signal of ICl molecules bound in van der Waals complexes.

free ICl molecules from the point of view of the orientation process (different rotational dynamics and probably higher rotational temperature) and they also contribute to the photodissociation process. This contribution cannot be always described by the axial recoil approximation and even if the complexes are well oriented, the corresponding photodissociation signal will carry a weaker anisotropy. However, the nonlinear behavior of the signal with the applied field is very well reproduced.

Using this fit, we deduced the ratio between the probabilities of finding the molecules parallel and antiparallel to the static electric field $W(\theta=0)/W(\theta=\pi)$. At the highest electric field (7 MV/m) we obtained a value of 1.84 for this ratio. Such a strong orientation of the molecular axis will be useful for reaction dynamics experiments.

7. Conclusion

In this paper, we have discussed the orientation of diatomic molecules by an intense electric field, with some emphasis on the nonlinear effects. We have then discussed the optimization of an oriented beam of ICl seeded in argon and we have shown that, because of clustering, the optimum is reached for large nozzle diameters and low source pressure. We have built such a beam and characterized its properties by LIF. The orientation of ICl was tested by a photodissociation experiment, made with a CW laser at 488 nm, an efficient choice to prevent electrical breakdown in the high voltage condenser.

The orientation signal is described carefully by a Monte Carlo modelization of the experiment. This modelization has been able to reproduce very well the observed signal and its nonlinear dependence with the applied field, but the deduced rotational distributions differ noticeably from the one measured directly by LIF. This discrepancy is probably due to the presence of van der Waals complexes of ICl in the beam: their orientation process and their rotational temperature are not known and possibly very different from the one of free ICl molecules and they contribute to the photodissociation signal.

Finally, this experiment provides two results: (1) a direct measurement of the sign of the dipole moment of ICl in the X state, found to be I^+Cl^- as expected, and (2) from our fit to the experimental data, we can deduce the maximum value of the ratio $W(\theta=0)/W(\theta=\pi) = 1.84$ (where $W(\Omega)$ is the distribution of the molecular axis). Clearly a strong orientation of ICl has been achieved.

Acknowledgment. We thank R. N. Zare for a very stimulating discussion, H. J. Loesch and S. Stolte for very helpful information, and J. C. Loison and A. Durand for their collaboration on this work in its early phase. The experimental setup owes much to the skill of A. Pellicer, P. Paquier, M. Gianesin, and P. Laflou. The financial support of our laboratory by Region Midi Pyrénées is gratefully acknowledged.

References and Notes

(1) Loesch, H. J.; Remscheid, A. *J. Chem. Phys.* **1990**, *93*, 4779−4790.
(2) Friedrich, B.; Herschbach, D. R. *Z. Phys. D.* **1991**, *18*, 153−161.
(3) Loesch, H. J.; Remscheid, A. *J. Phys. Chem.* **1991**, *95*, 8194−8200.
(4) Loesch, H. J.; Moller, J. *J. Chem. Phys.* **1992**, *97*, 9016−9030.
(5) Loesch, H. J.; Moller, J. *J. Phys. Chem.* **1993**, *97*, 2158−2166.
(6) Friedrich, B.; Rubahn, H. G.; Sathyamurthy, N. *Phys. Rev. Lett.* **1992**, *69*, 2487.
(7) Friedrich, B.; Herschbach, D. R. *Nature* **1991**, *353*, 412−414.
(8) Rost, J. M.; Griffin, J. C.; Friedrich, B.; Herschbach, D. R. *Phys. Rev. Lett.* **1992**, *68*, 1299−1302.
(9) Block, P. A.; Bohac, E. J.; Miller, R. E. *Phys. Rev. Lett.* **1992**, *68*, 1303−1306.
(10) Friedrich, B.; Herschbach, D. R.; Rost, J.-M.; Rubahn, H.-G.; Renger, M.; Verbeek, M. *J. Chem. Soc. Faraday Trans.* **1993**, *89*, 1539−1549.
(11) Durand, A.; Loison, J. C.; Vigué, J. *J. Chem. Phys.* **1994**, *101*, 3514−3519.
(12) Durand, A.; Loison, J. C.; Vigué, J. *C. R. Acad. Sci. Paris* **1994**, *319*, 739−744.
(13) Wu, M.; Bemish, R. J.; Miller, R. E. *J. Chem. Phys.* **1994**, *101*, 9447−9456.
(14) Bemish, R. J.; Bohac, E. J.; Wu, M.; Miller, R. E. *J. Chem. Phys.* **1994**, *101*, 9457−9468.
(15) Bazalgette, G.; White, R.; Loison, J. C.; Trénec, G.; Vigué, J. *Chem. Phys. Lett.* **1995**, *244*, 195−198.
(16) Bernstein, R. B.; Choi, S. E.; Stolte, S. *J. Chem. Soc., Faraday Trans. 2* **1985**, *85*, 1097−1113.
(17) Omont, A. *Prog. Quantum Electron.* **1977**, *5*, 69−138.
(18) Broyer, M.; Gouédard, G.; Lehmann, J. C.; Vigué, J. *Adv. Atom. Mol. Phys.* **1976**, *12*, 165.
(19) Loison, J. C.; Durand, A.; Bazalgette, G.; White, R.; Audouard, E.; Vigué, J. *J. Phys. Chem.* **1995**, *99*, 13591−13596.
(20) Bulthuis, J.; VanLeuken, J. J.; VanAmerom, F.; Stolte, S. *Chem. Phys. Lett.* **1994**, *222*, 378−386.
(21) Herbst, E.; Steinmetz, W. *J. Chem. Phys.* **1972**, *56*, 5342−5346.
(22) Hedderich, H. G.; Bernath, P. F.; McRae, G. A. *J. Mol. Spectrosc.* **1992**, *155*, 384−392.
(23) Durand, A.; Loison, J. C.; Vigué, J. *J. Chem. Phys.* **1997**, *106*, 477−484.
(24) Wannier, G. H. *Statistical Physics*; J. Wiley & Sons: New York, 1966.
(25) Bulthuis, J.; VanLeuken, J. J.; Stolte, S. *J. Chem. Soc., Faraday Trans.* **1995**, *91*, 205−214.
(26) VanLeuken, J. J.; Bulthuis, J.; Stolte, S.; Loesch, H. J. *J. Phys. Chem.* **1995**, *99*, 13582−13590.
(27) Friedrich, B.; Pullman, D. P.; Herschbach, D. R. *J. Phys. Chem.* **1991**, *95*, 8118−8129.
(28) Latham, R. V. *High voltage vacuum insulation: the physical basis*; Academic Press: London, 1981.
(29) Calder, G. V.; Giauque, W. F. *J. Phys. Chem.* **1965**, *69*, 2443.
(30) Lamoreaux, R. H.; Giauque, W. F. *J. Phys. Chem.* **1969**, *73*, 755.
(31) Beijerinck, H. C. W.; Verster, N. F. *Physica* **1981**, *111c*, 327.
(32) DePaul, S.; Pullman, D.; Friedrich, B. *J. Phys. Chem.* **1993**, *97*, 2167−2171.
(33) Toennies, J. P.; Winkelmann, K. *J. Chem. Phys.* **1977**, *66*, 3965−3979.
(34) Keil, D.; Lubbert, A.; Schugerl, K. *J. Chem. Phys.* **1983**, *79*, 3845−3850.
(35) Hansen, S. G.; Thompson, J. D.; Kennedy, R. A.; Howard, B. J. *J. Chem. Soc., Faraday Trans.* **1982**, *78*, 1293−1310.
(36) Wang, J.; Shamamian, V. A.; Thomas, B. R.; Wilkinson, J. M.; Riley, J.; Giese, C. F.; Gentry, R. *Phys. Rev. Lett.* **1988**, *60*, 696.

(37) Brusdeylins, G.; Toennies, J. P.; Vollmer, R. Presented at the 8th European Conference on Dynamics of Molecular Collisions; Molec VIII, 1990, Bernkastel-Kues.
(38) Meyer, H. D. Bildung von Dimeren in Edelgas-Duesenstrahlen. Thesis, Georg-August-Universitaet Goettingen, M. P. I., 1978.
(39) Knuth, E. L. *J. Chem. Phys.* **1977**, *66*, 3515−3525.
(40) Vasile, M. J.; Stevie, F. A. *J. Chem. Phys.* **1981**, *75*, 2399−2405.
(41) Girard, B.; Billy, N.; Gouédard, G.; Vigué, J. *J. Chem. Phys.* **1988**, *88*, 2342−2354.
(42) Zalicki, P.; Billy, N.; Gouédard, G.; Vigué, J. *J. Chem. Phys.* **1993**, *99*, 6436−6448.
(43) DeVries, M. S.; VanVeen, N. J. A.; Hutchinson, M.; DeVries, A. E. *Chem. Phys.* **1980**, *51*, 159−168.
(44) Ni, C.-K.; Flynn, G. W. *Chem. Phys. Lett.* **1993**, *210*, 333.
(45) Tonokura, K.; Fujimura, S.; Saito, K. *J. Chem. Phys.* **1993**, *99*, 3461−3467.
(46) Seery, D. J.; Britton, D. *J. Phys. Chem.* **1964**, *68*, 2263.
(47) Dunn, M. H.; Ross, J. N. *Prog. Quantum Electron.* **1976**, *4*, 235.
(48) Moore, C. E. *Atomic Energy Levels*; U.S. Government Printing Office: Washington, DC, 1971; Vol. 1.
(49) King, G. W.; McFadden, R. G. *Chem. Phys. Lett.* **1978**, *58*, 119−121.
(50) Dagenais, M.; Johns, J. W. C.; McKellar, A. R. W. *Can. J. Phys.* **1976**, *54*, 1438.
(51) Messiah, A. *Mecanique Quantique*; Dunod: Paris, 1969; Vol. 2, Chapter 17.
(52) Cummings, F. E.; Klemperer, W. *J. Chem. Phys.* **1974**, *60*, 2035−2039.
(53) Zare, R. N.; Herschbach, D. R. *Proc. IEEE* **1963**, *51*, 173.
(54) Zare, R. N. *J. Chem. Phys.* **1967**, *47*, 204.
(55) Zare, R. N. *Chem. Phys. Lett.* **1989**, *156*, 1−6.
(56) Taatjes, C. A.; Janssen, M. H. M.; Stolte, S. *Chem. Phys. Lett.* **1993**, *203*, 363−370.
(57) Center, R. E.; Mandl, A. *J. Chem. Phys.* **1972**, *57*, 4104−4105.
(58) Drawin, H. W. *Z. Phys.* **1961**, *164*, 513−521.
(59) Rosenblum, B.; Nethercot, J. A. H.; Townes, C. H. *Phys. Rev.* **1958**, *9*, 400.
(60) Ozier, I.; Crapo, L. M.; Ramsey, N. F. *J. Chem. Phys.* **1968**, *49*, 2314.
(61) Meerts, W. L.; DeLeeuw, F. H.; Dymanus, A. *Chem. Phys.* **1977**, *22*, 319−324.
(62) Townes, C. H.; Shawlow, A. L. *Microwave Spectroscopy*; McGraw-Hill: New York, 1955.
(63) Nair, K. P. R.; Hoeft, J.; Tiemann, E. *Chem. Phys. Lett.* **1979**, *60*, 253.
(64) Tiemann, E. *J. Mol. Struct.* **1983**, *97*, 331−345.
(65) Gouédard, G.; Billy, N.; Girard, B.; Vigué, J. *J. Phys. 2* **1992**, *2*, 813−825.
(66) Western, C. M.; Barney, W. S.; Clement, S. G.; Slotterback, T. J.; Janda, K. *Z. Phys. D.* **1996**, *36*, 273−283.
(67) Gripp, J.; Dreizler, H.; Gadhi, J.; Wlodarczak, G.; Legrand, J.; Burie, J.; Demaison, J. *J. Mol. Spectrosc.* **1988**, *129*, 381−387.
(68) Yokozeki, A.; Muenter, J. S. *J. Chem. Phys.* **1980**, *72*, 3796.
(69) Haberland, H.; Buck, U.; Tolle, M. *Rev. Sci. Instrum.* **1985**, *56*, 1712−1716.